



Citation for published version:

Johnston, N 2012, 'The transmission line method for modelling laminar flow of liquid in pipelines', Proceedings of the Institution of Mechanical Engineers, Part I: Journal of Systems and Control Engineering, vol. 226, no. 5, pp. 586-597. <https://doi.org/10.1177/0959651811430035>

DOI:

[10.1177/0959651811430035](https://doi.org/10.1177/0959651811430035)

Publication date:

2012

Document Version

Peer reviewed version

[Link to publication](#)

University of Bath

General rights

Copyright and moral rights for the publications made accessible in the public portal are retained by the authors and/or other copyright owners and it is a condition of accessing publications that users recognise and abide by the legal requirements associated with these rights.

Take down policy

If you believe that this document breaches copyright please contact us providing details, and we will remove access to the work immediately and investigate your claim.

The Transmission Line Method for Modelling Laminar Flow of Liquid in Pipelines

D N Johnston

Department of Mechanical Engineering, University of Bath, BA2 7AY

Summary

The transmission line method (TLM) is a very efficient method for dynamic modelling of flow in pipelines, and uses delay elements to represent wave propagation. In this paper an existing TLM model is investigated and shown to have some deficiencies. Some adjustments are proposed to avoid these deficiencies and enhance the transient and steady state accuracy. Very good agreement is obtained between this adjusted TLM and an analytical model. The model has been implemented in simulation of a number of highly dynamic systems, and has been found to be robust and reliable.

1. Introduction

Several techniques are available for dynamic modelling of laminar flow in pipelines. These include the Method of Characteristics (MOC) [1, 2], the lumped element method (LEM) [3], the finite element method (FEM) [4], various modal approximation (MA) methods [5, 6], and the Transmission Line Model (TLM) [7, 8, 9]. In the simulation of many fluid systems, the dynamics of the flow in pipelines is not important and simpler models can be used, resulting in simpler, faster and often more reliable simulations. However for some systems involving rapid dynamics or long pipelines, wave transmission effects become significant and more sophisticated models need to be used.

The MOC can be an extremely accurate method and can give results that are virtually indistinguishable from analytical solutions. In its basic form it is only suitable for fixed time step solvers and constant properties, although it can be used with variable time steps and variable properties if combined with an interpolation technique [1]. This introduces additional complexity and some numerical error in the form of artificial damping and smoothing. The MOC is used in the 'Flowmaster' simulation package [10].

The LEM takes the form of a series of lumped parameter resistor/inductor/capacitor (RLC) networks [3]. It is a simple method to understand and implement, and is very flexible in that variable properties and cavitation can be implemented. The FEM is a similar technique with similar advantages and disadvantages. At present many system simulation programs, such as Amesim [11] and SimHydraulics [3], use LEM and FEM models, and have a range of models of varying complexity. Multiple element models of these types are known to have limited accuracy for very rapid transients and may introduce unrealistic oscillations in some situations. They may also be very inefficient [12, 13].

The MA methods can be very accurate and are compatible with variable time step solvers, but are only suitable for fixed parameters and linear behaviour. MA methods are not widely used at present for fluid lines in commercial simulation packages.

The TLM is a very efficient technique for modelling transmission line problems [7, 8, 9]. It makes use of the inherent delay in transmission of pressure and flow from one end of the line to the other. In some respects the method is very similar to the MOC; in the MOC, the line is split up into short elements and pressure and flow values propagate from one node to the next over one timestep. In the TLM, the line is not subdivided but pressure and flow (or other variables) at each end are stored for a

number of timesteps. The variables (pressure and flow, or equivalent) at a new timestep are calculated from the variables at the other end delayed by a period of time. Importantly, the TLM is compatible with variable timestep integrators as interpolation can be used between previous data points. This means it can be incorporated readily into system models. Like the MA methods, it is restricted to fixed parameters and linear behaviour, but is believed to be more computationally efficient [13]. Because the pipe ends are separated by delays it is very well suited to parallel computation [14, 15].

Previous TLM models [8, 9] have been found to have some deficiencies. It was known that the TLM was unable to predict the shape of the initial transient in response to a step change at high damping levels, although this would be an insignificant effect in most cases. Perhaps more importantly, it will be shown later that the method gives an incorrect equivalent capacitance and inertance. The incorrect capacitance means that the pressure rise in response to an injection of fluid into a closed-ended tube will be inaccurate. The incorrect inertance means that the rate of change of flow in response to a change in pressure difference will be inaccurate.

The aims of this paper are to investigate in detail a previous TLM model, and to correct some of the deficiencies of this model.

2. Existing Transmission Line Method

A pipeline can be represented by the transmission matrix [16] given by equations (1) and (2).

$$\begin{pmatrix} P_1 \\ Q_1 Z_c \end{pmatrix} = \begin{pmatrix} t_{11} & t_{12} \\ t_{21} & t_{22} \end{pmatrix} \begin{pmatrix} P_2 \\ Q_2 Z_c \end{pmatrix} = \begin{pmatrix} \cos\left(\frac{\omega L}{c} \sqrt{N}\right) & -j\sqrt{N} \sin\left(\frac{\omega L}{c} \sqrt{N}\right) \\ \frac{j}{\sqrt{N}} \sin\left(\frac{\omega L}{c} \sqrt{N}\right) & -\cos\left(\frac{\omega L}{c} \sqrt{N}\right) \end{pmatrix} \begin{pmatrix} P_2 \\ Q_2 Z_c \end{pmatrix} \quad (1)$$

$$Z_c = \frac{\rho c}{A} \quad (2)$$

N is a frequency dependent function that depends on the type of friction model that is used [17]. This equation can be implemented readily in the frequency domain, but it is more difficult to implement in the time domain and approximations are generally needed. The TLM is a method to approximate this equation in the time domain.

In the absence of friction ($N=1$), the TLM is extremely simple and can be implemented using delays and algebraic equations. When friction is included, it becomes more complicated and approximations are needed, largely because N is complex and frequency dependent. Care has to be taken to ensure that the correct steady state pressure drop is predicted by the model as well as the correct damping of transients. Krus *et al.* [8] represented the equations by a block diagram similar to that shown in Figure 1. The characteristic values C_1 and C_2 are related to the pressure and flowrate by equations (3) and (4).

$$P_1 = C_1 + Z_c Q_1 \quad (3)$$

$$P_2 = C_2 + Z_c Q_2 \quad (4)$$

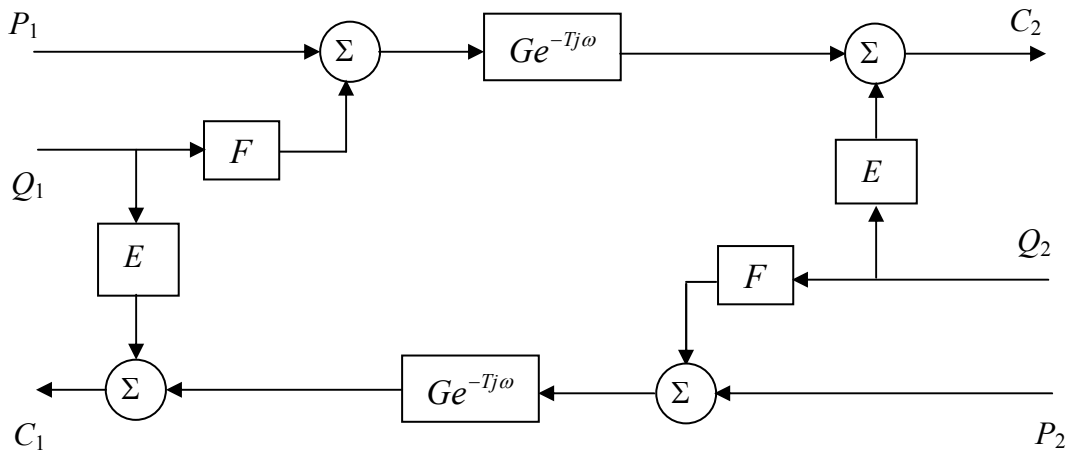


Figure 1 Block diagram for transmission line model

The block diagram shown in figure 1 can be combined with additional blocks representing equations (3) and (4) to obtain various combinations of pressures and flows as inputs or outputs to the model.

2.1 Exact model

The block diagram in figure 1 is an exact representation of the analytical transmission matrix, equation (1), if the terms are as follows [8].

$$E = Z_c(\sqrt{N} - 1) \quad (5)$$

$$F = Z_c\sqrt{N} \quad (6)$$

$$G = e^{-Tj\omega(\sqrt{N}-1)} = e^{-\beta j\alpha(\sqrt{N}-1)} \quad (7)$$

$$\alpha \text{ is the non-dimensional frequency, } \alpha = \frac{r^2 \omega}{\nu}, \quad (8)$$

$$\text{and } \beta \text{ is the dissipation number, } \beta = \frac{\nu L}{cr^2} = \frac{\nu T}{r^2}. \quad (9)$$

If quasi-steady laminar resistance is assumed, N is given by equation (10).

$$N = 1 + \frac{8}{j\alpha} \quad (10)$$

A more accurate model takes into account the velocity profile across the radius of the tube. The velocity profile varies with frequency [17] and the effect of this is commonly known as ‘unsteady’ or ‘frequency dependent’ friction. Including this effect and assuming laminar flow but neglecting thermal effects, N is given by the equation

$$N = \frac{1}{1 - \frac{2 J_1(z)}{z J_0(z)}} \text{ where } z = j\sqrt{j\alpha}. \quad (11)$$

2.2 Krus *et al.*'s approximation

Krus *et al.* [8] developed a model whose block diagram is as shown in Figure 1. Neglecting unsteady friction, the filters E and G were approximated to simple transfer functions. F was simply a constant.

$$E(j\omega) = \frac{R}{\kappa j\omega T + 1}, \text{ where } R = \frac{8\rho\nu L}{\pi r^4}. \quad (12)$$

κ is an empirical factor. Krus *et al.* proposed that $\kappa = 1.25$.

$$\text{Using non-dimensional terms, } E(j\alpha) = \frac{8\beta\rho c}{A(\kappa\beta j\alpha + 1)} \quad (13)$$

$$F = Z_C \quad (14)$$

$$G(j\omega) = \frac{\kappa j\omega T e^{\frac{RA}{2\rho c}} + 1}{\kappa j\omega T + 1} \quad (15)$$

$$\text{or } G(j\alpha) = \frac{\kappa\beta j\alpha e^{-4\beta} + 1}{\kappa\beta j\alpha + 1} \quad (16)$$

Equations (13) and (14) are not good approximations to the exact terms, equations (5) and (6), which both tend to infinity at low frequency. However this is not necessarily of direct importance, as it is the overall response of the approximated model that is important.

There are some constraints that need to be met. Equation (17) must be satisfied in order to give the correct pressure drop for a given flowrate in the steady state, and equation (18) must be satisfied for steady state continuity. These conditions are met by Krus *et al.*'s approximations.

$$F(0) - E(0) = Z_C - R = Z_C(1 - 8\beta) \quad (17)$$

$$G(0) = 1 \quad (18)$$

2.3 Approximation to unsteady friction

Trikha [18] developed a method for approximating unsteady laminar friction based on simple weighting functions, for use with the MOC. This is a flexible and efficient method which can be use to approximate a variety of transfer functions. Kagawa [19], Suzuki *et al.* [20], Taylor *et al.* [4] and Johnston [9] developed this method further. This method has also been applied to unsteady turbulent flow [4, 21, 22, 23], and to flexible hoses [24].

In their TLM model, Krus *et al.* [8] included an additional filter term in G to represent unsteady friction. They used a simple first-order lag which needed to be ‘tuned’ to give satisfactory results. Johnston [9] incorporated Trikha’s weighting function method into the TLM. The effect of unsteady friction on E and F was neglected.

Johnston [9] defined a friction function H , where $H = j\alpha(N-1)$. From equation (11), the analytical expression for H is

$$H = \frac{j\alpha}{\left[\frac{z J_0(z)}{2 J_1(z)} - 1 \right]} \quad (19)$$

Johnston approximated the friction function H by a sum of weighting functions, as follows:

$$H \approx 8 + 4 \sum_{i=1}^k \left(\frac{m_i j\alpha}{n_i + j\alpha} \right). \quad (20)$$

To develop an approximation for G , an approximation for $\sqrt{N}-1$ is needed. Provided that $\frac{H}{j\alpha}$ is small (which is true except for low frequencies), this can be approximated using the binomial series to

$$\sqrt{N}-1 = \sqrt{1 + \frac{H}{j\alpha}} - 1 \approx \frac{H}{2j\alpha}. \quad (21)$$

Substituting this approximation into equation (7),

$$G = e^{-(\beta j \alpha (\sqrt{N}-1))} \approx e^{-\frac{\beta H}{2}}. \quad (22)$$

Using the approximation for H given by equation (20), G can be approximated to

$$G \approx e^{-\frac{\beta}{2} \left[8 + 4 \sum_{i=1}^k \left(\frac{m_i j \alpha}{n_i + j \alpha} \right) \right]} = G_1 G_2 \quad (23)$$

$$\text{where } G_1 = e^{-4\beta} \quad (24)$$

$$\text{and } G_2 = e^{-\left(2\beta \sum_{i=1}^k \left(\frac{m_i j \alpha}{n_i + j \alpha} \right) \right)}. \quad (25)$$

At low frequency the true function for G , equation (7), tends towards an asymptotic value of 1. However the approximation, equation (23), has an asymptotic value of $e^{-4\beta}$ and this will cause flow continuity errors. To overcome this problem, the same function for G_1 can be used as for steady friction, that is,

$$G_1(j\alpha) = \frac{\kappa \beta j \alpha e^{-4\beta} + 1}{\kappa \beta j \alpha + 1}. \quad (26)$$

This is asymptotic to 1 at low frequencies and $e^{-4\beta}$ at high frequencies, as required.

Equation (25) for G_2 cannot easily be transformed to the time domain. Provided that the exponent is small, G_2 can be further approximated to a form that can be transformed easily to the time domain. Johnston [9] proposed equation (27), which is called ‘model 1’ in the current paper. The values of m_i and n_i are given in table 1.

The terms form geometric series except for the first two m terms.

$$G_2 = 1 - 2\beta \sum_{i=1}^k \left(\frac{m_i j \alpha}{n_i + j \alpha} \right). \quad (27)$$

$$\text{This is based on the expansion } e^{-x} = 1 - x + \frac{x^2}{2} - \frac{x^3}{3!} + \dots \quad (28)$$

Table 1 Terms used in friction approximation

term i	m_i	n_i
1	2.2457	42.849
2	6.8400	385.60 ($= n_1 \times 9$)
$i = 3$ to 8	$m_i = m_{i-1} \times 3$	$n_i = n_{i-1} \times 9$

Unfortunately the magnitude of G_2 can exceed 1 at high frequency. The model can then become unstable and sharp spikes occur which increase in amplitude. This is most likely to occur for large values of β . This problem can be avoided by using fewer terms k , or artificially reducing the higher values of m_i so that $\beta \sum_{i=1}^k m_i < 1$.

These steps may ensure stability at the expense of accuracy.

To avoid this instability problem without impairing accuracy, two alternative approximations are introduced: model 2 (equation 29) and model 3 (equation 31). In these models $|G_2|$ cannot exceed 1.

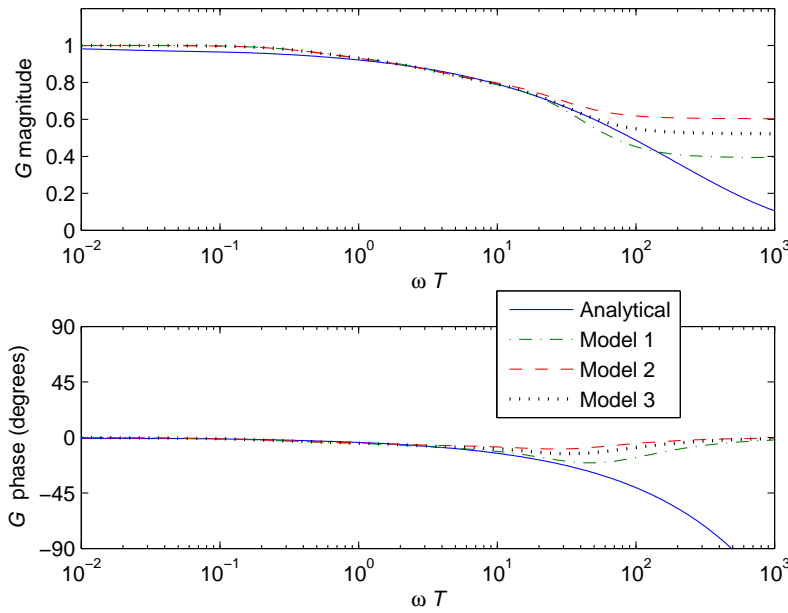
$$\text{Model 2: } G_2 = \frac{1}{1 + 2\beta \sum_{i=1}^k \left(\frac{m_i j \alpha}{n_i + j \alpha} \right)} \quad (29)$$

$$\text{This is based on } e^{-x} = \frac{1}{e^x} = \frac{1}{1 + x + \frac{x^2}{2} + \frac{x^3}{3!} + \dots} \quad (30)$$

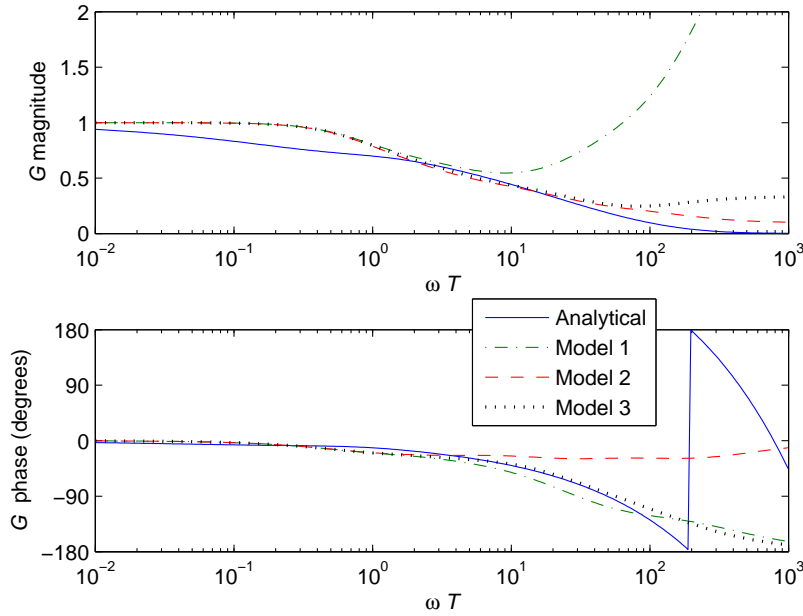
$$\text{Model 3: } G_2 = \frac{1 - \beta \sum_{i=1}^k \left(\frac{m_i j \alpha}{n_i + j \alpha} \right)}{1 + \beta \sum_{i=1}^k \left(\frac{m_i j \alpha}{n_i + j \alpha} \right)} \quad (31)$$

$$\text{This is based on } e^{-2x} = \frac{e^{-x}}{e^x} = \frac{1 - x + \frac{x^2}{2} - \frac{x^3}{3!} + \dots}{1 + x + \frac{x^2}{2} + \frac{x^3}{3!} + \dots}. \quad (32)$$

The three approximations to G ($=G_1G_2$) and the analytical function G are plotted against ωT in figure 2. Eight terms were used in the approximation ($k = 8$). For small β , figure 2(a), the approximations are good for $\omega T < 10$, but the phase deviates at higher frequencies. For large β , figure 2(b), the approximations are less good, and for model 1 the magnitude of G exceeds 1 at high frequencies. Model 2 gives a better match to the magnitude, and the magnitude never exceeds 1 regardless of the number of terms k , but the phase lag is under-predicted. Model 3 gives the best overall match and the magnitude is always less than 1. Nonetheless the match becomes poor when the theoretical magnitude becomes less than 0.5.



(a) $\beta = 0.01$



(b) $\beta = 0.1$

Figure 2 Approximations to G for basic TLM

The three weighting function models can be implemented readily using summations of simple first-order transfer functions. For example a block diagram for model 3 is shown in figure 3. Model 1 would be implemented using the left-hand half only of this block diagram, and model 2 would be implemented using the right-hand half only, in both cases multiplying the numerator of the weighting functions by two. Models 2 and 3 may result in implicit algebraic equations (known as an ‘algebraic loop’ in Matlab Simulink). To avoid the algebraic loop, an artificial low-pass filter transfer function can be added to the forward path, with a bandwidth greater than that of the highest weighting function. This is shown in the dotted box in figure 3, with a break frequency of twice the highest weighting function. It should have a negligible effect on the accuracy but may affect the simulation speed slightly. Another way of eliminating the algebraic loop is to expand the complete weighting function (equation 29 or 31) to form a rational function (that is, a ratio of two polynomials). This can be done by pre-calculation before the simulation starts.

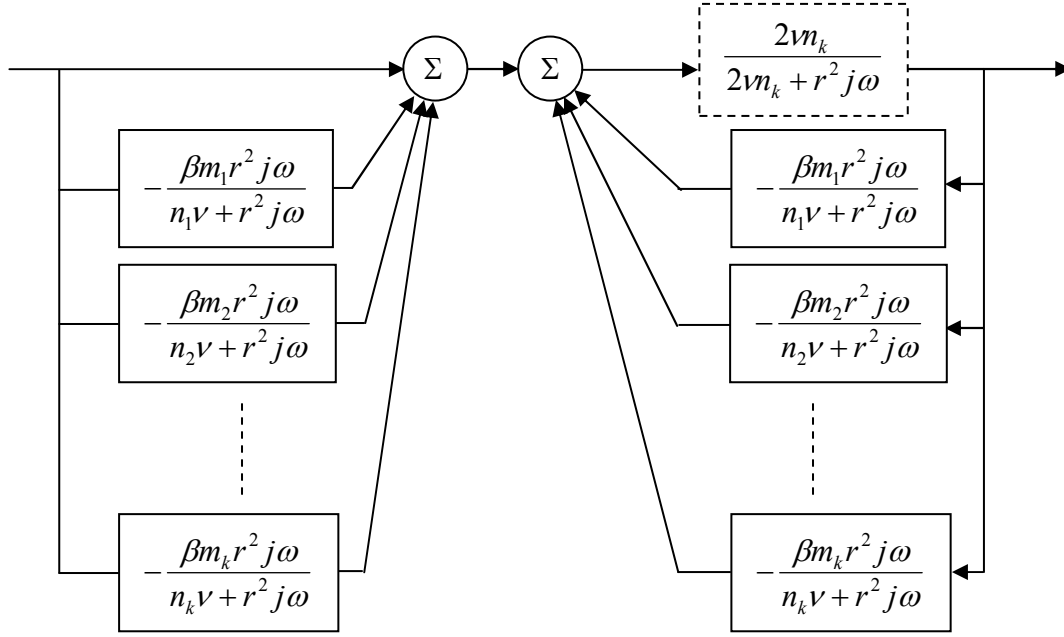


Figure 3 Implementation of G_2 , model 3

2.4 Transient simulation results

The simulations presented here and in section 3 were done using a pipe length of 45 m, a diameter of 13 mm, fluid density of 870 kg/m³ and a bulk modulus of 1.5182 GPa, with a range of viscosities to give the required values of β according to equation (9). All results shown here are non-dimensionalised, and they only vary depending on β ; the same results would be obtained if different pipe dimensions and fluid properties were used but the same values of β were maintained. Results in section 2 are referred to as using the ‘uncorrected TLM’ to distinguish them from the ‘corrected TLM’ in section 3.

Figure 4 shows results for a step change in flow at the upstream end and a fixed pressure at the downstream end, for the three different approximations to G_2 . Only results for $\beta = 0.1$ are shown as for smaller values of β the differences are negligible. In this case the number of terms $k = 4$. The results are compared with an analytical solution obtained using an inverse Fourier transform of the model [4]. The

error is defined as the absolute difference between the TLM and analytical result, relative to the magnitude of the initial pressure step. There are very small differences between the three models, and no significant improvement in the overall accuracy by using model 3, even though the accuracy of G itself is improved. Spikes are apparent in the results for models 1 and 3; model 2 is the smoothest. For these reasons model 2 is considered to be the preferred model and is used for subsequent results.

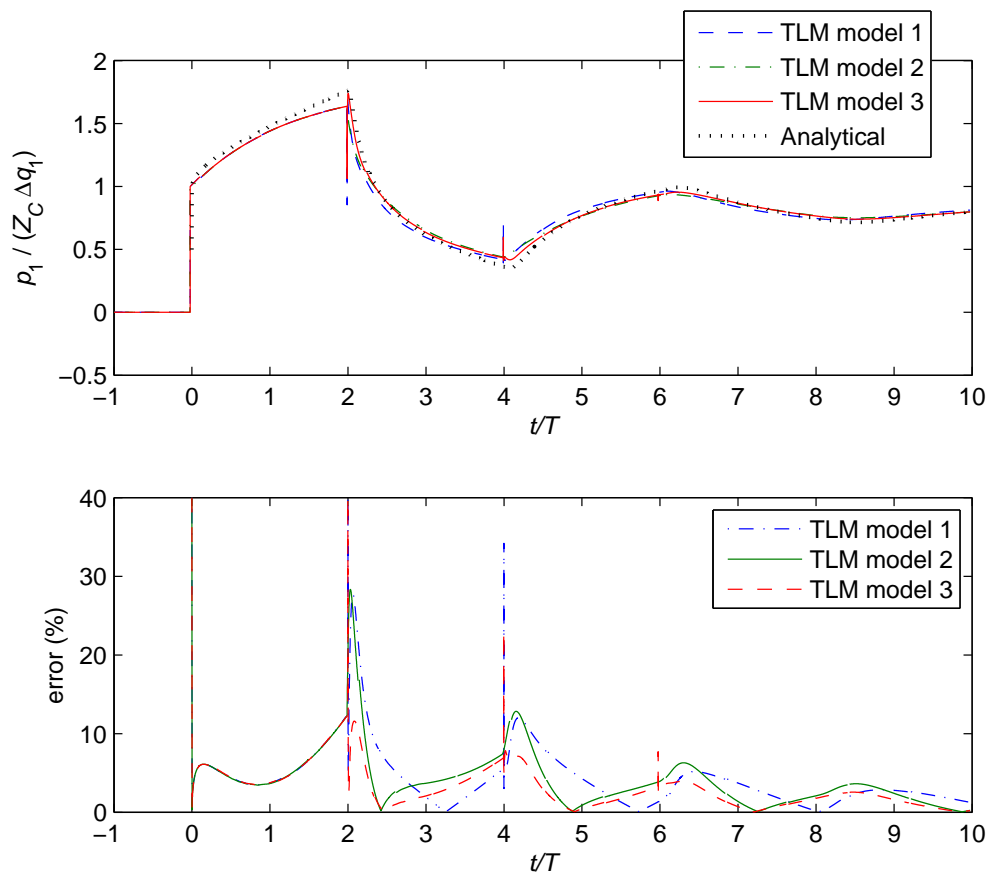
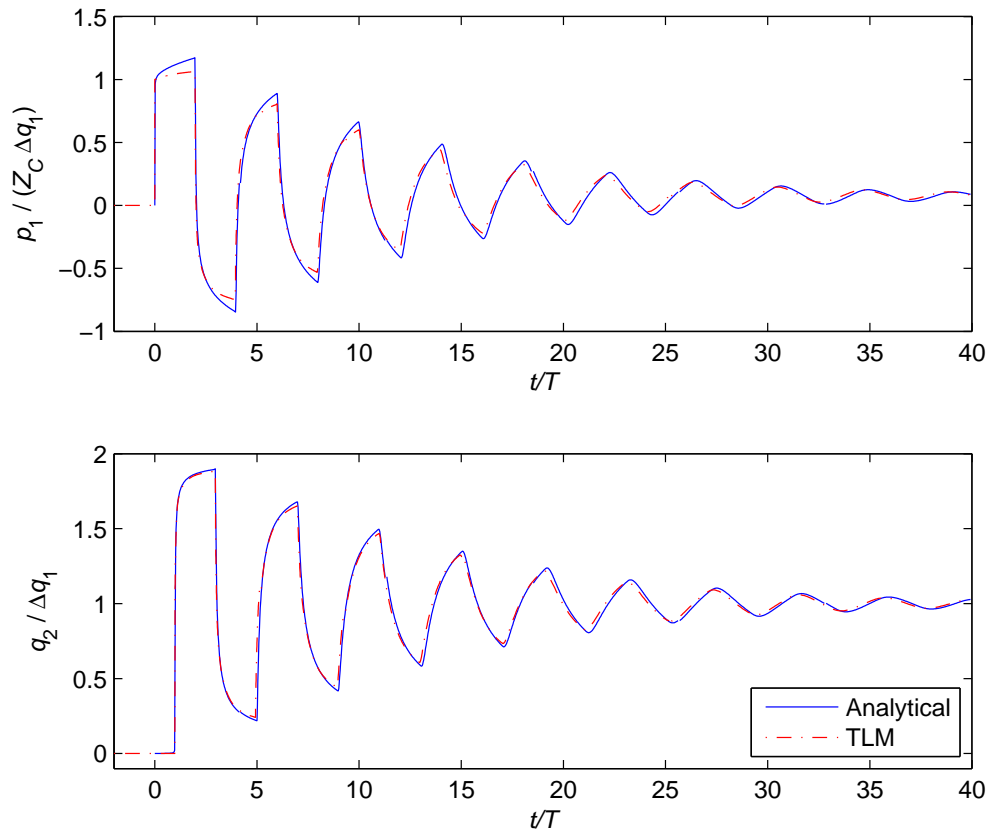


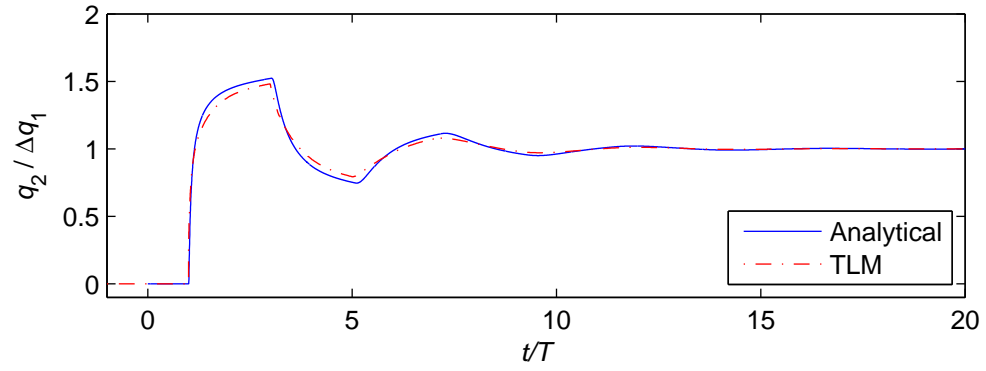
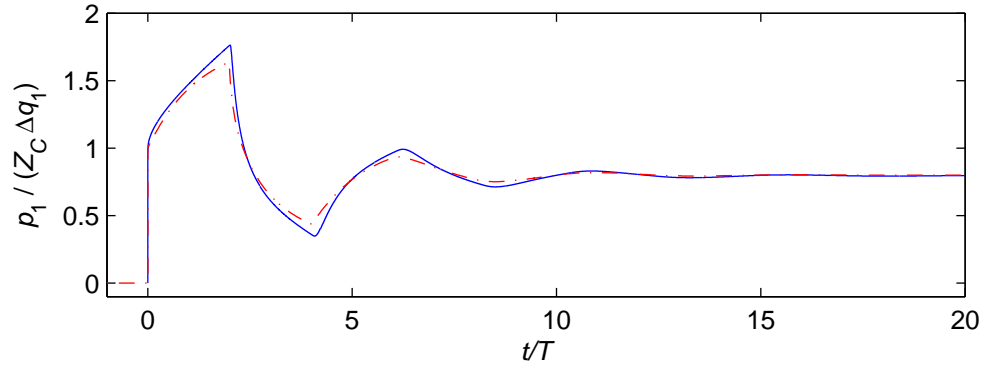
Figure 4 Time domain results for a step change in upstream flow with a fixed downstream pressure, $\beta = 0.1$, with different unsteady friction models, uncorrected TLM

Figure 5 shows analytical predictions and TLM results, for a step change in flow at the upstream end and a fixed pressure at the downstream end. The agreement in

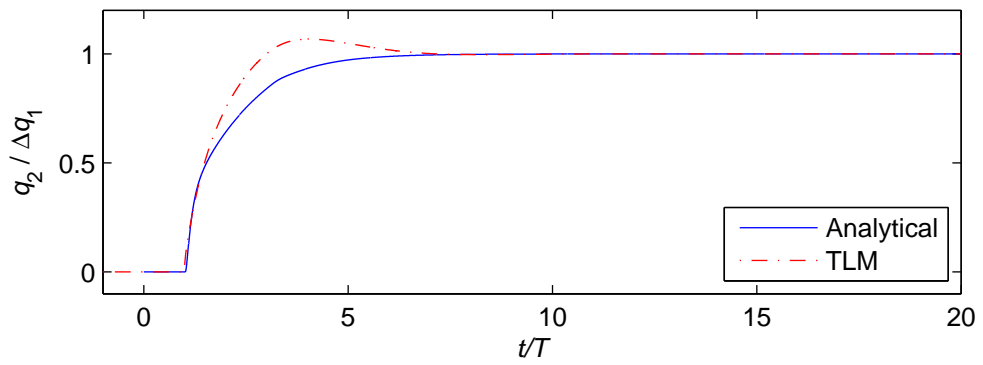
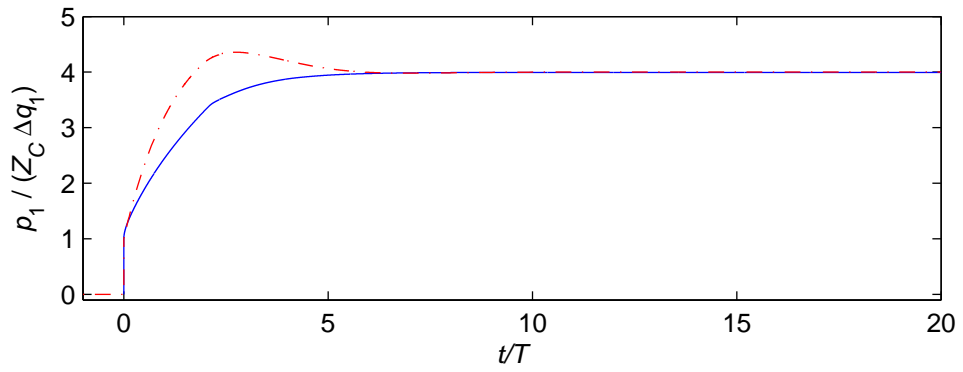
figure 5(a) and (b) is quite good, especially for the flow predictions. Figure 5(c) shows an overshoot for $\beta = 0.5$. The agreement was found to be good for $\beta < 0.3$.



(a) $\beta = 0.01$



(b) $\beta = 0.1$



(c) $\beta = 0.5$

Figure 5 Time domain results for a step change in upstream flow with a fixed downstream pressure, uncorrected TLM

Figure 6 shows the predicted pressure for a closed-ended line with a short pulse of flow at one end, for a range of values of β . The analytical response is also shown for $\beta = 0.1$. The non-dimensionalised pressure $\frac{pV}{B\Delta V}$ should tend to 1 after the transient dies away. The TLM significantly underestimates the pressure rise for low β and overestimates for high β . This indicates that the TLM model produces an error in the effective capacitance of the pipeline. This problem will be investigated in section 2.5.

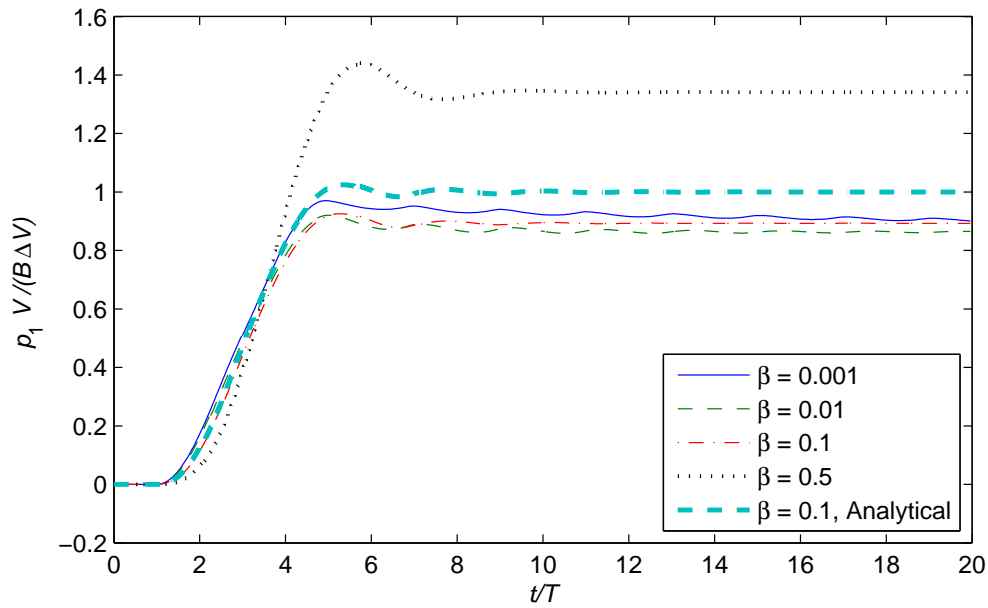


Figure 6 Predicted pressure (non-dimensionalised) for a flow pulse at one end with the other end blocked, uncorrected TLM

Figure 7 shows the response to a step change in upstream pressure, with a constant downstream pressure. Some difference in the response of the TLM model is apparent for $\beta = 0.01$, suggesting an inaccuracy in the effective inertance of the TLM model. The steady state pressure after the transient decays is predicted very accurately.

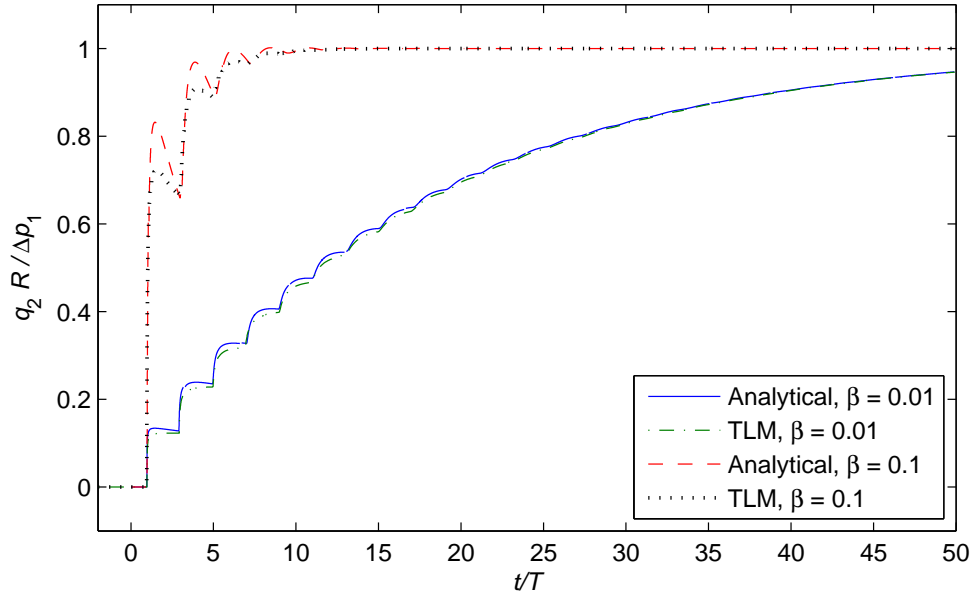


Figure 7 Predicted flowrate (non-dimensionalised) in response to a step change in pressure, with a fixed pressure at the other end, uncorrected TLM

2.4.1 Effect of inaccuracy in E and F

In the model, E has been approximated to a first-order lag, and it is assumed that $F = Z_C$. This may cause significant error as the theoretical value of $|\sqrt{N}|$ tends to infinity as $\omega \rightarrow 0$, regardless of whether unsteady friction is included, and so the theoretical magnitudes of E and F both tend to ∞ as $\omega \rightarrow 0$. If one considers an anechoic line or a very long line, a step change in flow should result in the pressure stepping up and then continuing to increase indefinitely as shown in the analytical prediction in figure 8 (the plot is zoomed in on the initial peak, and the pressure is initially zero, $p_1/Z_C \Delta q_1 = 0$ for $t < 0$). The response for any length should be identical to this anechoic line until the reflected wave causes a negative step change. As can be seen, the TLM model does not predict this correctly, and significantly under-estimates the pressure. The shape of the curve of the first pressure peak

predicted by the TLM differs according to the length of the pipeline. However until the first reflection occurs the length of pipeline should have no influence on the pressure. The reason that it does influence it in the TLM is that the approximated function for E depends on β (equation 13).

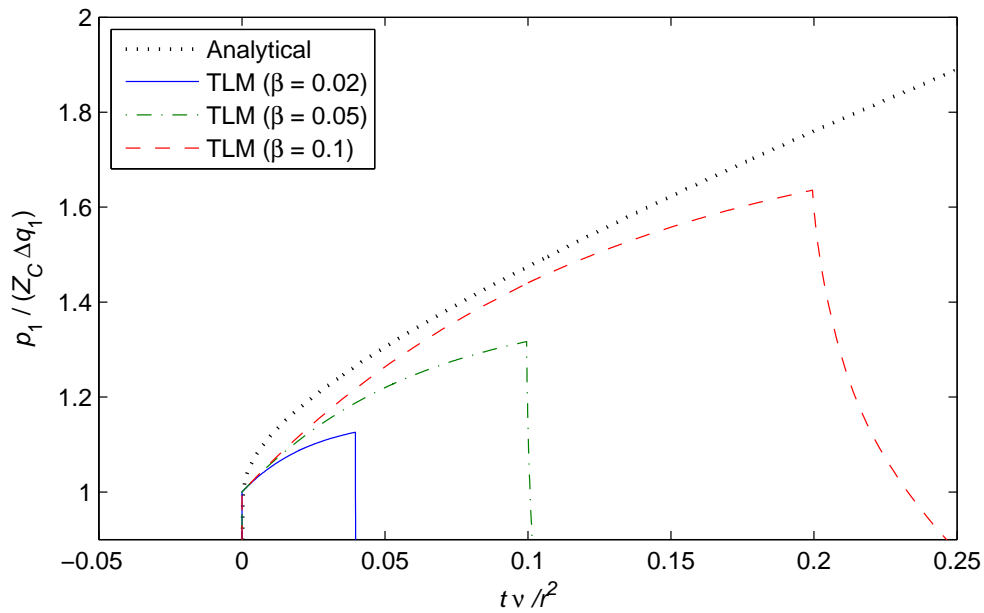


Figure 8 Pressure response to a step change in flow (comparison with analytical response of a very long or anechoic line), uncorrected TLM

2.5 Transmission Matrices

To determine the reasons for the inaccuracies in the TLM results, the transmission matrix obtained using the approximate equations in the frequency domain was investigated. The analytical transmission matrix is defined by equation (1). The transmission matrix terms for the TLM approximation were determined by setting different boundary conditions to the block diagram shown in figure 1. By setting P_2 to zero the relationship between P_1 and Q_2 gives t_{12} , and the relationship between Q_1 and Q_2 gives t_{22} . Similarly by setting Q_2 to zero, t_{11} and t_{21} can be found. These are given by equations (33) – (36).

$$t_{11} = \frac{(E + Z_C)G^{-1}e^{j\omega T} + FGe^{-j\omega T}}{(E + Z_C + F)} \quad (33)$$

$$t_{12} = \frac{(E + Z_C)^2 G^{-1}e^{j\omega T} - F^2 Ge^{-j\omega T}}{Z_C(E + Z_C + F)} \quad (34)$$

$$t_{21} = \frac{(Ge^{-j\omega T} - G^{-1}e^{j\omega T})Z_C}{E + Z_C + F} \quad (35)$$

$$t_{22} = -t_{11} \quad (36)$$

Figure 9 shows the theoretical and approximated transmission matrices.

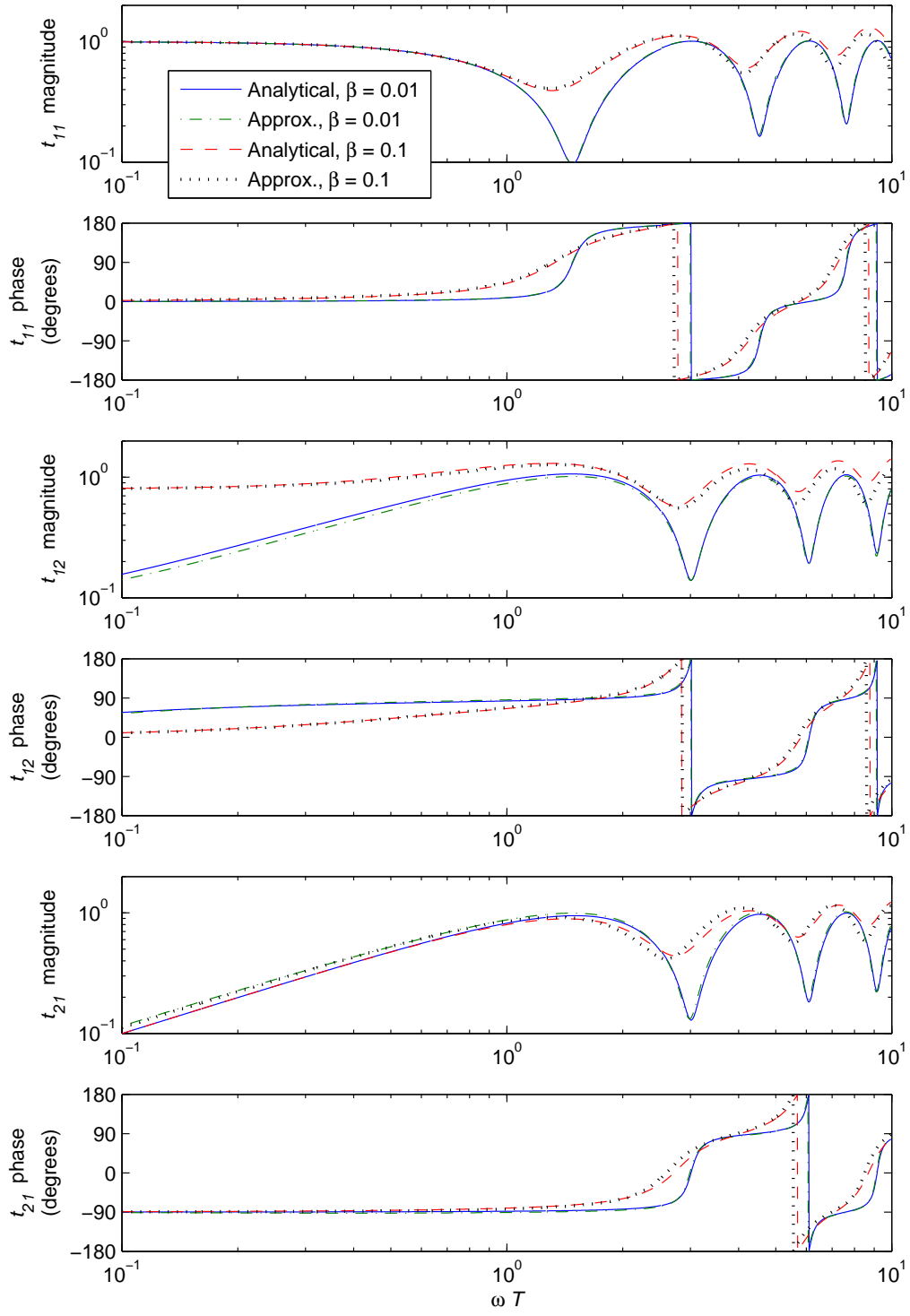


Figure 9 Transmission matrix terms, uncorrected TLM

The approximations are generally good for frequencies above the first modal frequency ($\omega T > \frac{\pi}{2}$) and small β , but slightly less good for large β . At low frequencies, the approximation to t_{11} is good (and identical to $-t_{22}$).

There is a small deviation in t_{12} below the first modal frequency but the lines converge at very low frequencies. This suggests that the effective inertance of the model is incorrect, which gives rise to the error in the rate of increase of flowrate in figure 7. The low-frequency asymptote for t_{12} governs the steady state pressure drop (since $P_1 = t_{12}Z_C Q_2$ if $P_2 = 0$), and the exact value is given by $t_{12} = 8\beta$. The low frequency asymptote of the approximate t_{12} (equation 34) is given by the equation

$$\frac{(E(0) + Z_C)^2 - F^2}{(E(0) + Z_C + F)Z_C} = \frac{(8\beta + 1)^2 - 1}{2 + 8\beta} = 8\beta. \quad (37)$$

This means that the model should give the correct steady state pressure drop and this is consistent with figure 7.

There is a small deviation in t_{21} below the first modal frequency and the two lines form parallel asymptotic straight lines. The low frequency asymptote for t_{21} governs the capacitance (since $Q_1 = \frac{t_{21}P_2}{Z_C}$ if $Q_2 = 0$). The capacitance is given by

$$\frac{t_{21}}{j\omega Z_C}. \text{ The exact } t_{21} \text{ term tends towards } t_{21} \rightarrow j\omega T \text{ as } \omega \rightarrow 0.$$

The low frequency asymptote for the approximated t_{21} term is given by equation (38). The unsteady friction model has a strong effect on the low frequency asymptote and introduces an additional error into the capacitance. This is an unintended side-

effect of the unsteady friction model, which was not expected to influence steady state behaviour.

$$t_{21} \rightarrow \frac{j\omega T \left(1 + \kappa [1 - e^{-4\beta}] + 2 \sum_{i=1}^k \frac{m_i}{n_i} \right)}{1 + 4\beta} \text{ as } \omega \rightarrow 0 \quad (38)$$

The error is shown in figure 10, for $k = 4$. The error is significant (up to 16%) even for very small dissipation number β . In some situations this may be important, and this is the cause of the errors in the steady state pressure in figure 6. Krus *et al.*'s simplified model [8] of unsteady friction also suffers from this problem.

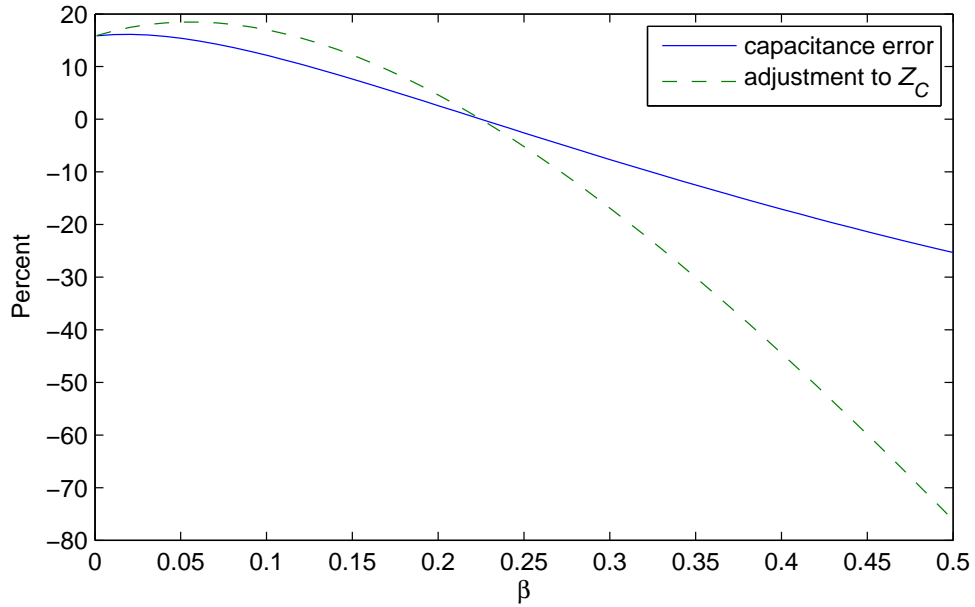


Figure 10 Error in capacitance and adjustment to Z_C

The low frequency response of t_{12} depends on the resistance and inertance of the line. As can be seen in figure 9 the low frequency horizontal asymptote is correct, but the upward sloping section is incorrect in the model, suggesting an error in the inertance. This error is caused by the unsteady friction model, in a similar way to the capacitance error, and is the cause of the discrepancies in figure 8.

3. ‘Corrected TLM’ model with adjustment for capacitance

The error in the capacitance can be eliminated by adjusting the characteristic impedance using equation (39). The model with this adjustment applied is called the ‘corrected TLM’ here.

$$Z_C = \frac{\rho c}{A} \left(1 + \kappa [1 - e^{-4\beta}] + 2 \sum_{i=1}^k \frac{m_i}{n_i} - 4\beta \right) \quad (39)$$

The percentage adjustment to Z_C is shown in figure 10, for $k = 4$. The magnitude of the adjustment is less than 20% for values of β less than 0.3, but increases for higher values of β .

The error in the inductance, and the effect of the capacitance correction on the inductance, are more difficult to quantify. The low frequency response of t_{12} can be represented as an effective resistance and inductance in series:

$$z_{12} = R_E + j\omega L_E. \quad (40)$$

The effective inductance and resistance vary with frequency, and for high dissipation numbers the effect of the inductance is masked by the high resistance. An estimate of the error in the inductance can be obtained by considering the frequency at which the phase of t_{12} passes through 45° , that is, where $\omega = \frac{R_E}{L_E}$. Figure 11 shows

the percentage error in this frequency, relative to the frequency for the analytical model. When the capacitance correction is used the error is reduced for $\beta < 0.05$, but not eliminated.

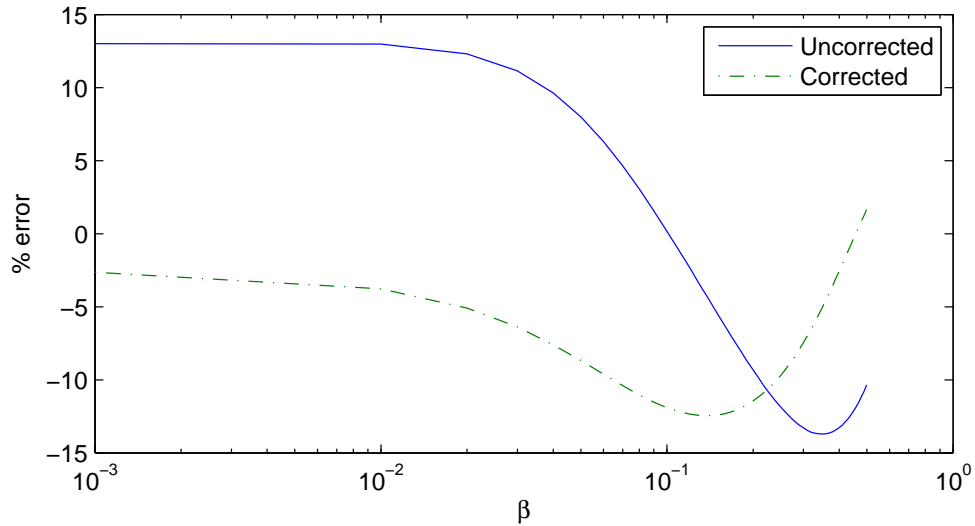
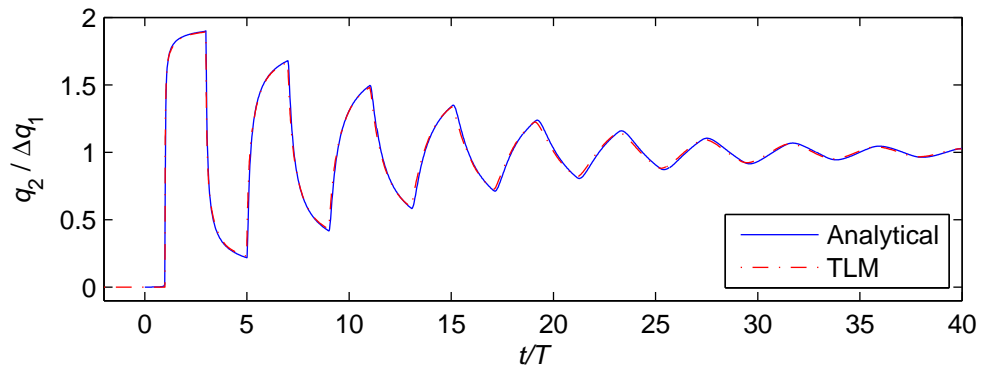
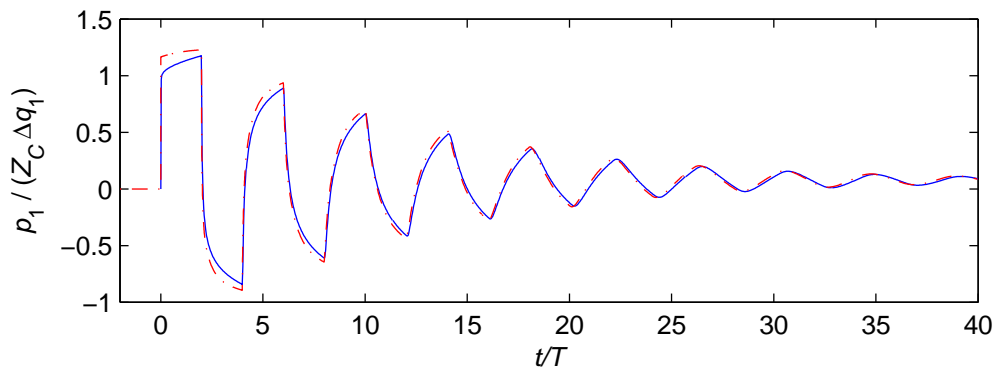
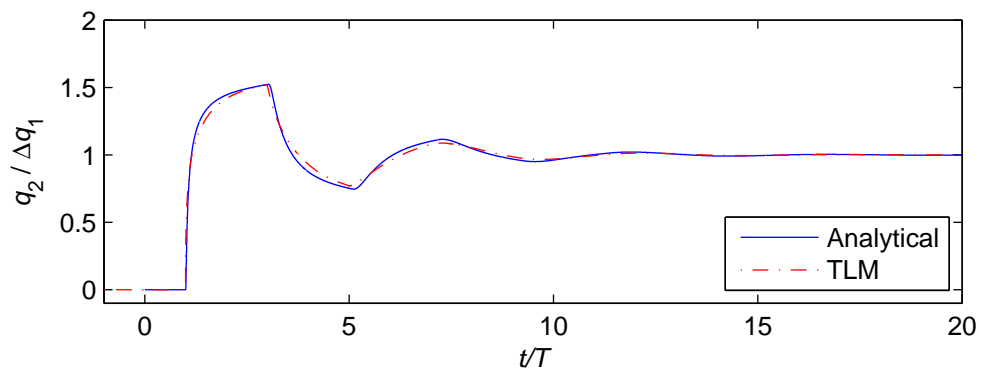
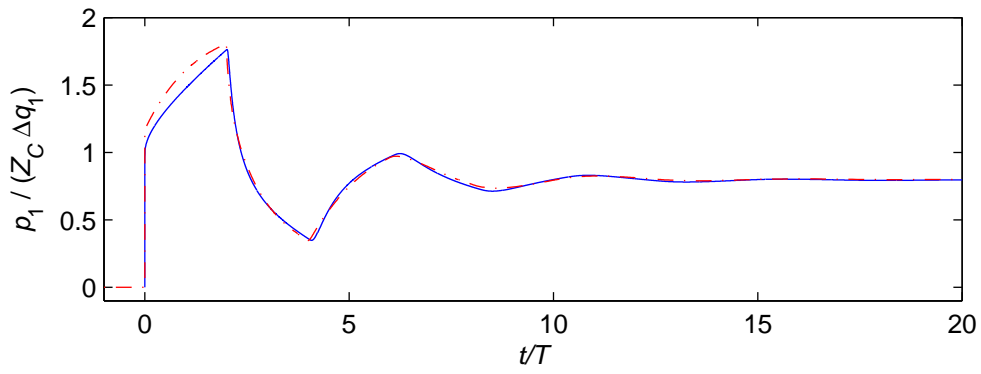


Figure 11 Error in frequency at which phase of $t_{12} = 45^\circ$

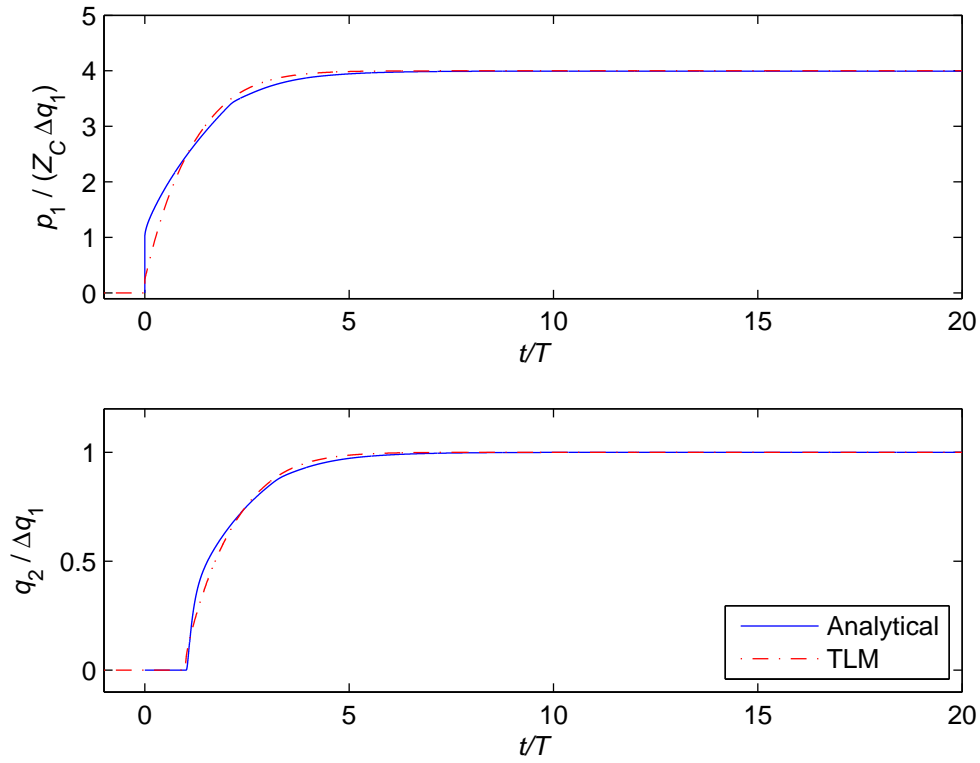
Figure 12 shows analytical predictions and TLM results with the capacitance correction applied, for a step change in flow at the upstream end and a fixed pressure at the downstream end. The agreement is good. The pressure peaks are over-estimated slightly for $\beta = 0.01$ and 0.1 , but for $\beta = 0.5$ the agreement is better than for the uncorrected model, figure 5(c). The flow results are the same as for the uncorrected model.



(a) $\beta = 0.01$



(b) $\beta = 0.1$



(c) $\beta = 0.5$

Figure 12 Time domain results for a step change in upstream flow with a fixed downstream pressure, corrected TLM

The initial pressure peaks for different values of β are compared with the analytical pressure rise in figure 13. Whilst the uncorrected TLM model (figure 8) underestimated the pressure rise slightly, the corrected TLM model overestimates the rise slightly for these values of β . The initial edge of the pressure step is overestimated by about 15% in these cases, but the peak pressure at the trailing edge is overestimated by about 1 – 2%. For higher values of β the initial edge of the pressure step is under-estimated as shown in figure 12(c).

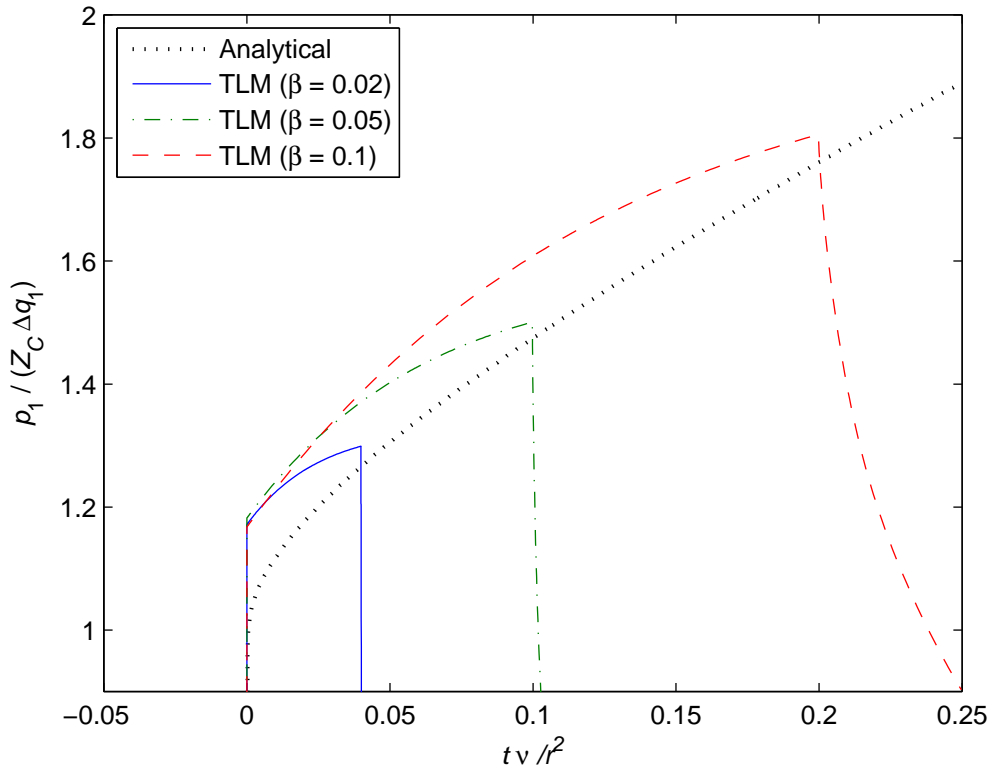


Figure 13 Pressure response to a step change in flow (comparison with analytical response of a very long or anechoic line), corrected TLM

Figure 14 shows the predicted pressure for a closed-ended line with a short pulse of flow at one end, for a range of values of β . The analytical response is also shown for $\beta = 0.1$ only. The corrected TLM estimates the steady state pressure rise correctly in all cases. However for very small dissipation number, $\beta = 0.001$, there is a small overshoot and slow decay towards the correct value. This is because the time constant for the first term of the unsteady friction approximation is equal to $\frac{T}{n_1 \beta}$ seconds, and becomes large for small β .

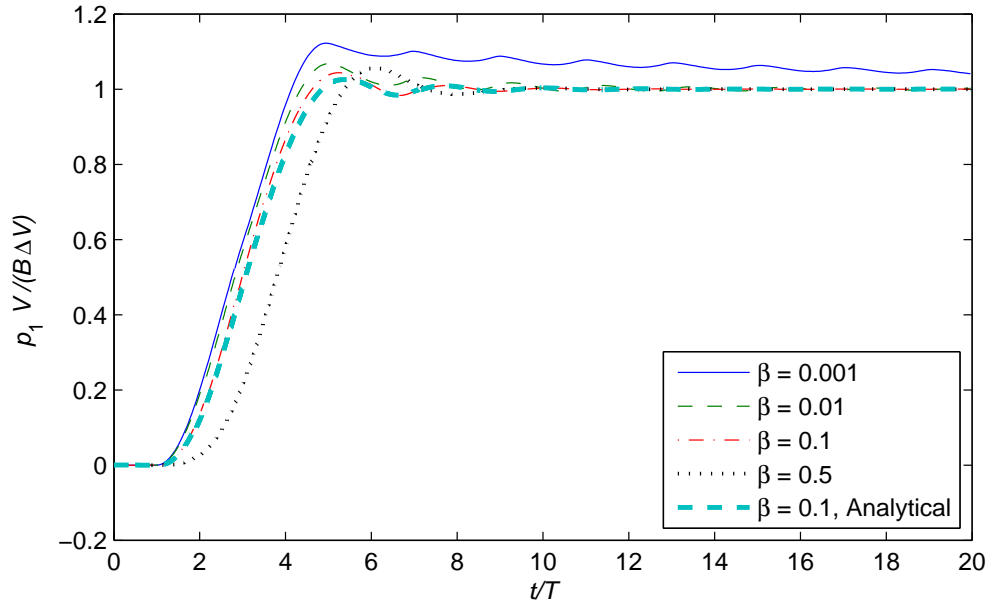


Figure 14 Predicted pressure (non-dimensionalised) for a flow pulse at one end with the other end blocked, corrected TLM

Figure 15 shows the response to a step change in upstream pressure, with a constant downstream pressure. Compared to figure 7 the rate of pressure rise is greatly improved. For $\beta = 0.1$ the pressure rise is very rapid and the results are dominated by the high resistance, although the pulsations are underestimated slightly at this condition. The steady state pressure after the transient decays is predicted very accurately.

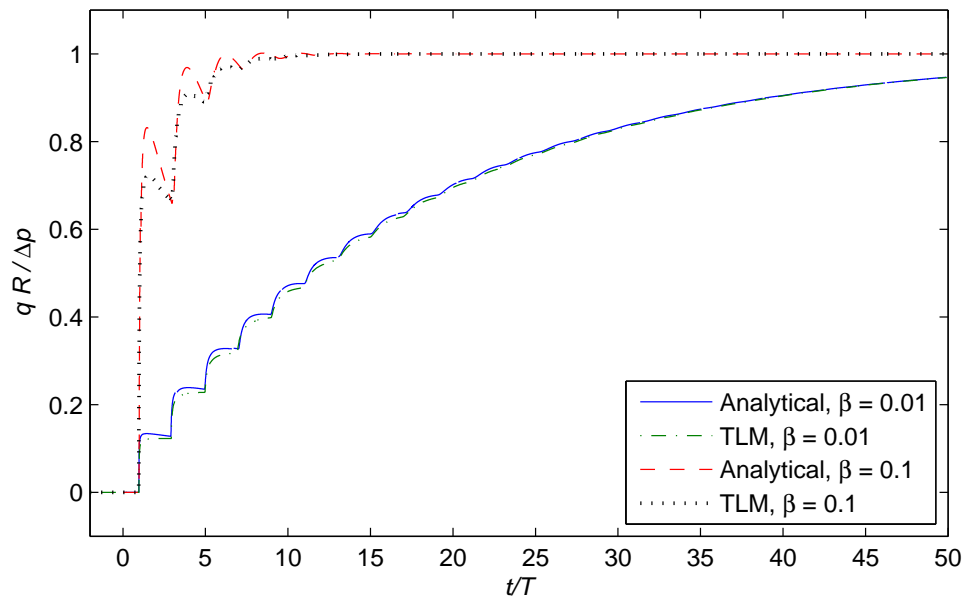


Figure 15 Predicted flowrate (non-dimensionalised) in response to a step change in pressure, with a fixed pressure at the other end, corrected TLM

4. Discussion

In section 2, the previous TLM model has been investigated in detail. The limitations of it have been explored, and a small improvement to eliminate a potential instability has been developed. The model has been found to give errors in the effective capacitance and inertance, and in the amplitude and shape of the step response.

In section 3, a simple adjustment to the model has been proposed to correct for the error in the capacitance. This also reduces but does not eliminate the error in the inertance. The adjustment improves the results in most cases. The error in the inertance may be important in some situations, for example when modelling a Helmholtz damper where the inertance of the tube is important, and this should be borne in mind.

For β less than about 0.001, the time constants for the first terms of the unsteady friction model become very long compared to the wave delay time. This has been found to cause a slight overshoot followed by slow decay of the results towards the steady state value after a transient. In this situation a very simple undamped model may be sufficient, as damping in adjoining components is likely to be far more significant. Alternatively the unsteady friction may be removed, or just the first one or two weighting terms of the unsteady friction could be removed.

The model does not work well for $\beta > 0.5$, which may occur for combinations of very long lines with small diameter and high viscosity. However wave effects may not be important for these very high damping conditions, and simpler lumped parameter models may be used. Alternatively multiple TLM models can be connected in series to represent very high values of β .

The TLM model has been applied extensively to switched hydraulic systems [25]. These systems use fast-acting valves in a form of pulse-width modulation. A long ‘inertance’ tube may be connected to the valve, and the momentum of the fluid in this tube enables step-up or step-down conversion of pressure or flow. The dynamic behaviour of the inertance tube has a very important effect on the result. The TLM model has been used to represent this inertance tube and has proved to be very reliable, robust and efficient. The models for the valve, inertance tube and other components have been linked together using small compressible volumes, partly to represent real fluid volumes at the interfaces but also to eliminate implicit algebraic equations. The selection of the size of these volumes is a compromise, in that a larger than real volume will affect the accuracy whereas a small volume may increase the simulation run-time. However provided that a suitable ‘stiff’ solver is used, it has

been found that sufficiently small volumes (typically 0.1% to 1% of the pipeline volume) may be used without affecting accuracy or run-times significantly.

The increased accuracy of the proposed TLM model compared to the previous model of Krus *et al.* [8] is gained at the expense of more computational effort. Krus *et al.*'s model required 6-8 states, whilst the proposed model typically requires 14 states (for $k = 4$). Both models require two delays. The proposed model may become numerically stiff and computationally slow if the number of terms k is large, as the highest terms (with high index i) in the summations in equations (27), (29) or (31) may have very small time constants.

As discussed here, the corrected TLM has a few limitations, with small errors in the inductance, small errors in the pulsation magnitude and shape, and possible overshoot and slow drift for low dissipation number. These errors are relatively minor and may be acceptable in most situations. However an enhanced TLM model is being developed which addresses these limitations at the expense of increased complexity. It is hoped that this will be published in the near future.

The TLM model can be extended to turbulent flow. However this is more complex as additional factors need to be considered – Reynolds number and roughness. Initial results have been encouraging. It may require that the coefficients are time-dependent as Reynolds number will change during a transient simulation.

5. Conclusions

An existing transmission line model has been found to be inaccurate under certain circumstances. The reasons for these inaccuracies have been analysed. The method has been modified to enhance the transient and steady state accuracy, with the result that very good agreement is obtained between this corrected TLM and an analytical model.

The TLM models have been implemented in Matlab Simulink and are available for downloading [26]. They have been used in various system models and have been found to be reliable and efficient. They are easy to link into system simulations using variable time step solvers. However it is recognised that more testing in actual applications is needed, and the experience of other users will be valuable in establishing the performance and ease of use of the TLM models in practice.

References

- [1] Wylie, E.B, *Fluid Transients*, revised edition, New York & London, McGraw Hill, 1978
- [2] Vitkovsky, J., Lambert, M., Simpson, A. and Bergant, A., Advances in unsteady friction modelling in transient pipe flow, BHR Group conference on Pressure Surges, Safe Design and Operation of Industrial Pipe Systems, BHR Group Conf. Series, Pub. No. 39, 2000
- [3] Mathworks product documentation: segmented pipeline, <http://www.mathworks.it/help/toolbox/physmod/hydro/ref/segmentedpipeline.html>, accessed June 2011
- [4] Taylor, S.E.M., Johnston, D.N. and Longmore, D.K., Modelling of transient flows in hydraulic pipelines, Proc. IMechE Pt I, vol. 211, no. I6, 1997, 447-456
- [5] Watton, J. and Tadmori, M.J., A comparison of techniques for the analysis of transmission line dynamics in electrohydraulic control systems. Applied Mathematical Modelling, vol. 12, Oct. 1988, 457-466.
- [6] Wongputorn, W., Hullender, D.A., and Woods, R.L., Rational polynomial transfer function approximations for fluid transients in lines, Proc. of ASME FEDSM'03, 4th ASME_JSME Joint Fluids Engineering Conference, FEDSM2003-45247, Honolulu, Hawaii, July 2003

- [7] Karam, J.T. and Leonard, R.G., A simple yet theoretically based time domain model for fluid transmission line systems, Trans. ASME, Journal of Fluids Engineering, vol. 95, Series I, No. 4, Dec 1973, pp498-504
- [8] Krus, P., Weddfelt, K. and Palmberg, J-O., Fast pipeline models for simulation of hydraulic systems, Journal of Dynamic Systems, Measurement and Control, Trans. ASME, vol. 116, no. 1, Mar, 1994, pp132-136
- [9] Johnston, D.N., Efficient methods for numerical modeling of laminar friction in fluid lines, Trans. ASME, Journal of Dynamic Systems Measurement and Control, vol. 128, no. 4, Dec. 2006, pp829-834
- [10] Dudlik, A., Schluter, S., Hoyer, N., Prasser H.-M., Pressure Surges - Experimental Investigations and Calculations with Software Codes Using Different Physical Models and Assumptions, 8th International Conference on Pressure Surges - Safe Design and Operation of Industrial Pipe Systems, The Hague, The Netherlands, 12-14 April 2000, BHR Group
- [11] Chapter 4: Selecting submodels for hydraulic lines. In: Amesim hydraulic library, Rev 8B, December 2008, LMS Imagine S.A.
- [12] Sanada, K, Richards, C.W., Longmore, D.K., Johnston, D.N., Burrows, C.R., Practical requirements for modelling the dynamics of hydraulic pipelines, 2nd JHPS Int. Symposium on Fluid Power, Tokyo, Sept. 1993
- [13] Soumelidis, M.I., Johnston, D.N., Edge, K.A., Tilley, D.G., A comparative study of modelling techniques for laminar flow transients in hydraulic pipelines, JFPS conf., Nov 2005
- [14] Burton J.D., Edge K.A. and Burrows CR, Modeling requirements for the parallel simulation of hydraulic systems, Journal of Dynamic Systems, Measurement and Control, vol. 116, 1994, pp137-145

- [15] Axin, M., Braun, R., Dell'Amico, A., Eriksson, B., Nordin, P., Petterson, K., Staak, I and Krus, P., Next generation simulation software using transmission line elements, Proceedings of Bath/ASME Symposium on Fluid Power and Motion Control 2010, Bath, 15-17 September 2010, University of Bath
- [16] Goodson, R.E. and Leonard, R.G., A survey of modeling techniques for fluid line transients, Trans. ASME, Jour. Basic Eng., June 1972, p474
- [17] Stecki, J.S. and Davis, D.C., Fluid transmission lines-distributed parameter models. Part 1: a review of the state of the art. Proc IMechE, vol. 200, no. A4, 1986, pp215-228.
- [18] Trikha, A.K., An efficient method for simulating frequency-dependent friction in transient liquid flow. Trans. ASME Journal of Fluids Engineering, March 1975, Series I, pp97-105.
- [19] Kagawa, T., Lee, I., Kitagawa, A. and Takenaka, T., High speed and accurate computing method of frequency-dependent friction in laminar pipe flow for characteristics method, Bull. JSME, vol. 49, no. 447, pp2638-2644
- [20] Suzuki K., Taketomi T., Sato S., Improving Zielke's method of simulating frequency-dependent friction in laminar liquid pipe flow, Journal of Fluids Engineering, Trans. ASME, vol. 113, Dec. 1991, pp569-573
- [21] Vardy, A.E. and Brown, J.M.B., Efficient approximation of unsteady friction weighting functions, Journal of Hydraulic Engineering, vol. 130, no. 11, 2004, pp1097-1107
- [22] Vítkovský J., Stephens M., Bergant A., Lambert M. and Simpson A., Efficient and accurate calculation of Zielke and Vardy-Brown unsteady friction in pipe transients, 9th International Conference on Pressure Surges, Chester, United Kingdom, 24–26 March 2004.

- [23] Johnston, D.N., Numerical modelling of unsteady turbulent flow in smooth-walled pipes, Proc. IMechE, Part C, Journal of Mechanical Engineering Science, vol 225, no. 7, 2011, pp1601-1615
- [24] Johnston, D.N., A time domain model of axial wave propagation in liquid-filled flexible hoses, Proc IMechE, part I, vol 220, no. 7, 2006, pp517-530
- [25] Johnston, D.N., A switched inertance device for efficient control of pressure and flow, Bath/ASME Symposium on Fluid Power and Motion Control, Hollywood, October 2009
- [26] Johnston, D.N., Pipeline models in Matlab Simulink, available from <http://people.bath.ac.uk/ensdnj/models>, accessed September 2011

Appendix 1: Nomenclature

A	Internal cross-sectional area
c	Speed of sound
$C_{1,2}$	Characteristic at end 1 and 2
E	Weighting function
F	Weighting function
G	Weighting function
G_1	Steady friction component of G
G_2	Unsteady friction component of G
H	Friction function
$J_{0,1}$	Bessel functions of the first kind
L	Length of pipeline
L_E	Effective inertance
m_i	Coefficient of weighting function
n_i	Coefficient of weighting function
N	Friction function
r	Internal radius of pipe
R	Resistance
R_E	Effective resistance

$p_{1,2}$	Pressure at end 1 and 2
$P_{1,2}$	Fourier transform of pressure at end 1 and 2
$q_{1,2}$	Flow into end 1 and 2
$Q_{1,2}$	Fourier transform of flow into end 1 and 2
$t_{11,12,21,22}$	Transmission matrix terms
T	Wave propagation time for pipeline
V	Fluid volume in pipeline
z	Complex non-dimensional frequency parameter
Z_C	Characteristic impedance
Δp	Pressure difference across ends of pipe
Δq	Magnitude of step change in flowrate
ΔV	Volume of fluid injected into pipe
α	Non-dimensional frequency
β	Dissipation number
κ	Empirical factor
ν	Kinematic viscosity
ρ	Fluid density
ω	Angular frequency